

## Consequences of a saturated convection electric field on the ring current

M. W. Liemohn,<sup>1</sup> J. U. Kozyra,<sup>1</sup> M. R. Hairston,<sup>2</sup> D. R. Weimer,<sup>3</sup> G. Lu,<sup>4</sup> A. J. Ridley,<sup>1</sup> T. H. Zurbuchen,<sup>1</sup> and R. M. Skoug<sup>5</sup>

Received 26 October 2001; revised 5 April 2002; accepted 10 April 2002; published 15 May 2002.

[1] Results from kinetic simulations of hot ion transport in the inner magnetosphere are used to show that the ring current energy content must have a nonlinear (asymptotic) coupling relationship to extreme solar wind conditions due to saturation of the near-Earth convection electric field  $E_{y,conv}$  (defined as a function of cross polar cap potential  $\Delta\Phi_{PC}$ ). This study examines the Bastille Day magnetic storm (July 14–17, 2000), where the z-component of the interplanetary magnetic field reached  $-58$  nT and the solar wind speed exceeded  $1100$  km  $s^{-1}$ . A large discrepancy in the modeled  $\Delta\Phi_{PC}$  confirms a nonlinear response of the high-latitude potential during this event. It is found that this nonlinearity of  $E_{y,conv}$  is necessary to obtain reasonable agreement between the simulation results and the observed geoeffectiveness (Dst) of the storm. *INDEX TERMS:* 2788 Magnetospheric Physics: Storms and substorms; 2784 Magnetospheric Physics: Solar wind/magnetosphere interactions; 2760 Magnetospheric Physics: Plasma convection

### 1. Introduction

[2] Knowing the geoeffectiveness of solar wind disturbances is a critical component of predicting space storms. A number of studies predict a linear relationship between interplanetary conditions and the cross polar cap potential difference  $\Delta\Phi_{PC}$ . *Burke et al.* [1999] gives a summary of these studies, ranging from the earliest using Atmospheric Explorer data [e.g., *Reiff et al.*, 1981] to recent analyses using Dynamics Explorer data [*Weimer*, 1996] and Defense Meteorological Satellite Program (DMSP) measurements [*Boyle et al.*, 1997]. Often, linear relationships were found between  $\Delta\Phi_{PC}$  and the y-component of the solar wind motional electric field  $E_{y,sw}$  (or the z-component of the interplanetary magnetic field  $B_{z,IMF}$ ).

[3] This linearity between conditions in the solar wind and near-Earth space has also been found by those attempting to predict “storm-time disturbance” index Dst. *Burton et al.* [1975] found a linear relationship between the growth rate of  $|Dst|$  and  $E_{y,sw}$ . Such a relationship is not surprising considering the many studies finding linear relationships between  $\Delta\Phi_{PC}$  and  $E_{y,sw}$ . Distributing the potential across lower latitudes means  $\Delta\Phi_{PC}$  must also be the cross magnetospheric potential difference  $\Delta\Phi_{MAG}$ . When mapped along field lines, the dawn-dusk convection electric field  $E_{y,conv}$  from this lower-latitude potential pattern drives the near-Earth plasma sheet through the inner magnetosphere, creating the stormtime ring current and therefore the Dst signatures. Thus, the coupling functions representing subauroral magnetospheric

dynamics should have the same dependence on the solar wind conditions as the high-latitude coupling functions.

[4] Nonlinear relationships of  $\Delta\Phi_{PC}$  to the solar wind have also been found. *Hill et al.* [1976] showed that the magnetic perturbation from region 1 currents alters the magnetic field topology at the subsolar reconnection zone, creating an upper bound on  $\Delta\Phi_{PC}$  (ionospheric drag [e.g., *Cole*, 1963]). *Siscoe et al.* [2001] showed that the *Hill et al.* [1976] relationship accurately predicts  $\Delta\Phi_{PC}$  as calculated by a sophisticated magnetohydrodynamic model under a variety of scenarios. The new W2K empirical model [*Weimer*, 2001] has a physically-based nonlinear dependence on  $B_{z,IMF}$ , now scaling primarily with  $E_{y,sw} B_{z,IMF}^{-1/3}$ . Based on results from several storms, the recent study of *Russell et al.* [2001] found that  $\Delta\Phi_{PC}$  becomes nonlinear for  $E_{y,sw}$  greater than a few mV  $m^{-1}$ .

[5] Because of the connection described above, the plasma in the inner magnetosphere should also exhibit a nonlinear (asymptotic) response to  $E_{y,sw}$ . Such a relationship, however, has not been shown. In fact, *Russell et al.* [2001] claim that the inner magnetosphere remains linearly coupled to  $E_{y,sw}$  throughout the  $E_{y,sw}$  range of their study (up to 24 mV  $m^{-1}$ ).

[6] In this letter, the issue of solar wind geoeffectiveness will be addressed by considering the inner magnetospheric response to extreme solar wind conditions. The Bastille Day Storm of July 14–17, 2000 (Bastille Day is July 14, the day the coronal mass ejection left the sun), will be examined because of its pathologically large  $B_{z,IMF}$  and  $E_{y,sw}$  and saturation of  $\Delta\Phi_{PC}$ . It is shown that, contrary to the assertion of *Russell et al.* [2001], the stormtime ring current also exhibits asymptotic nonlinearities in its magnitude.

### 2. Bastille Day Storm of 2000

[7] Figure 1 shows the unusual solar wind and geophysical characteristics of this storm. Two shocks hit the Earth, indicated in the plot by vertical dotted lines, with solar wind velocity jumps up to 770 km  $s^{-1}$  and 950 km  $s^{-1}$ , respectively (it then rose to 1100 km  $s^{-1}$ ). The solar wind dynamic pressure  $P_{sw}$  (Figure 1a), from the SWEPAM instrument on the ACE satellite, had large pulses in association with the shock fronts. Figure 1b shows ACE observations of  $B_{z,IMF}$ , with a southward perturbation ( $-14$  nT) after the first shock passage and a much larger excursion ( $-58$  nT) after the second shock. The magnetic field rotated from southward to northeastward (early on July 16) before settling back near zero late on July 16. Such large  $B_{z,IMF}$  and  $V_{sw}$  values yields an intense  $E_{y,sw}$  (Figure 1c), peaking at 59 mV  $m^{-1}$  around 2000 UT on July 15.

[8] This interplanetary disturbance caused a major magnetic storm in geospace. Large disturbances were recorded in the 3-h Kp index (Figure 1d) and the Dst index (Figure 1e). Also shown in Figure 1e are  $D_{MP}$  and  $Dst^*$  [e.g., *Kozyra et al.*, 1998],

$$D_{MP} = 15.5\sqrt{P_{sw}} \quad Dst^* = (Dst - D_{MP} - 20)/1.3$$

the contributions to Dst from the magnetopause currents and near-Earth currents, respectively (in nT). During storms, the largest contributors to  $Dst^*$  are the partial and symmetric ring currents in the inner magnetosphere [e.g. *Greenspan and Hamilton*, 2000].

<sup>1</sup>Space Physics Research Laboratory, University of Michigan, Ann Arbor, USA.

<sup>2</sup>Center for Space Science, University of Texas at Dallas, Richardson, USA.

<sup>3</sup>Mission Research Corporation, Nashua, New Hampshire, USA.

<sup>4</sup>High Altitude Observatory, NCAR, Boulder, Colorado, USA

<sup>5</sup>Los Alamos National Laboratory, New Mexico, USA.

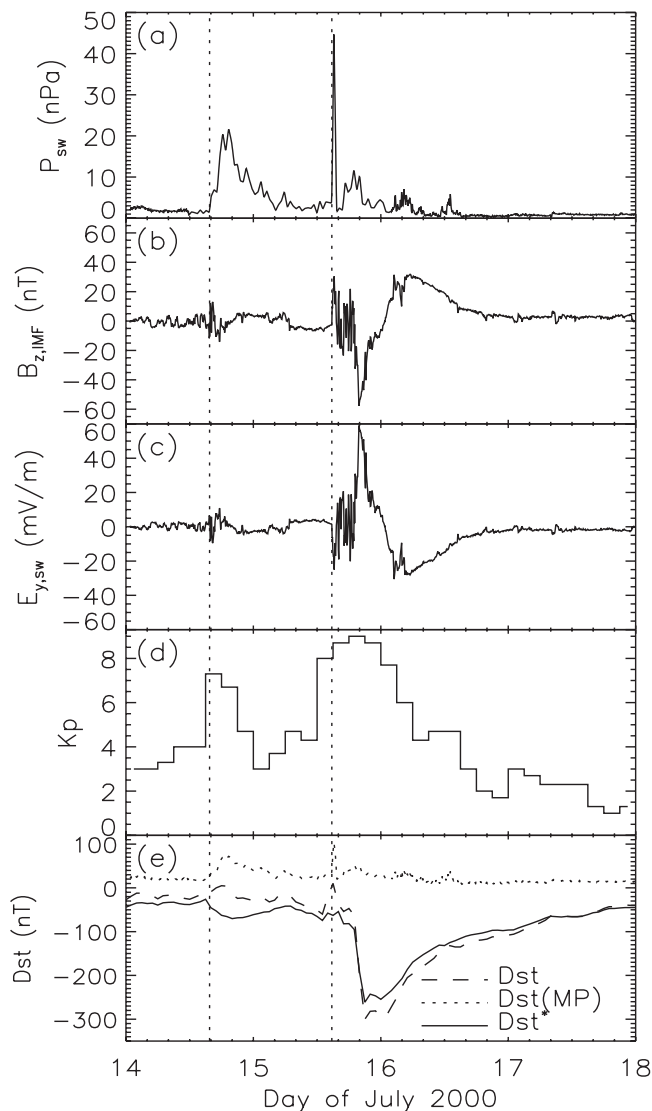


**Figure 1.** Solar wind and geophysical parameters during the Bastille Day storm. Shown here are (a)  $P_{sw}$ , (b)  $B_{z,IMF}$ , (c)  $E_{y,sw}$ , (d)  $Kp$ , and (e)  $Dst$  (dashed line), along with the magnetopause contribution (dotted line) and the inner magnetospheric contribution (solid line). The vertical dotted lines indicate the shock arrivals at Earth. The solar wind values have been propagated to the Earth with a time lag of  $\Delta t = \Delta x/V_{sw}$ .

$Dst^*$  reveals a moderate storm on July 14, with a  $-71$  nT minimum at 2000 UT, while the big event on July 15 has a  $Dst^*$  minimum of  $-261$  nT.

[9] The geophysical effects seen in Figure 1 are driven by intense magnetospheric convection. This flow was driven by the coupling of  $E_{y,sw}$  into the high-latitude ionosphere. The parameter of interest for this study is  $\Delta\Phi_{PC}$ , which, as stated above, is assumed equal to  $\Delta\Phi_{MAG}$ . Figure 2 shows several representations of  $\Delta\Phi_{PC}$ : from the W-96 model [Weimer, 1996]; from the W2K model [Weimer, 2001]; from the assimilative mapping of ionospheric electrodynamics (AMIE) inversion [Richmond and Kamide, 1988] of magnetometer data for this interval; and DMSP observations of  $\Delta\Phi_{PC}$  (from 4 satellites, using the method described by Rich and Hairston [1994] and Hairston and Heelis [1996], corrected up to 20% to account for the satellites not cutting through the high and low peaks of the potential pattern). Limitations to the validity of each of these techniques for determining

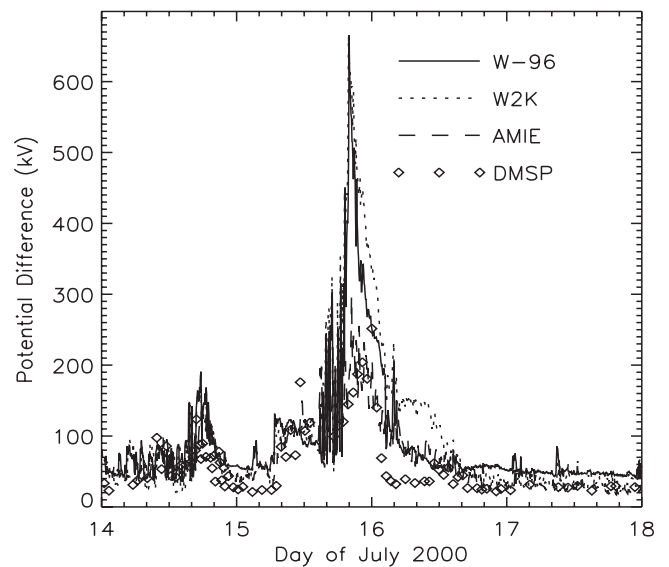


**Figure 2.** Cross polar cap potential differences for this period from the Weimer-96 and Weimer-2000 empirical models, an AMIE inversion of ground-based magnetometer data, and DMSP measurements.

$\Delta\Phi_{PC}$  are discussed in the listed citations. It is seen that both W-96 and W2K predict peak values over 650 kV. While it is not surprising for the “linear” W-96 model to produce such a large number, the W2K prediction also went abnormally large because of the cloud’s high speed. In contrast, the AMIE and DMSP  $\Delta\Phi_{PC}$  values never exceed 250 kV (except for 2 brief spikes late on July 15 for the AMIE results).

[10] Because the AMIE and DMSP  $\Delta\Phi_{PC}$  values are derived from ionospheric observations, it is thought that they more accurately represent the true  $\Delta\Phi_{PC}$  time series during the event. Figure 2 is consistent with the findings of Siscoe *et al.* [2001], who predict  $\Delta\Phi_{PC}$  saturation value of 256 kV at the extremum of the solar wind values on July 15. DMSP observations for March 31, 2001, which had very similar IMF conditions to the Bastille Day storm, confirm a saturated  $\Delta\Phi_{PC}$  during that storm’s extreme solar wind values [Hairston *et al.*, 2001].

[11] To quantitatively analyze the nonlinearity of this relationship, Figure 3 shows  $\Delta\Phi_{PC}$  versus  $E_{y,sw}$  for the W-96 and AMIE

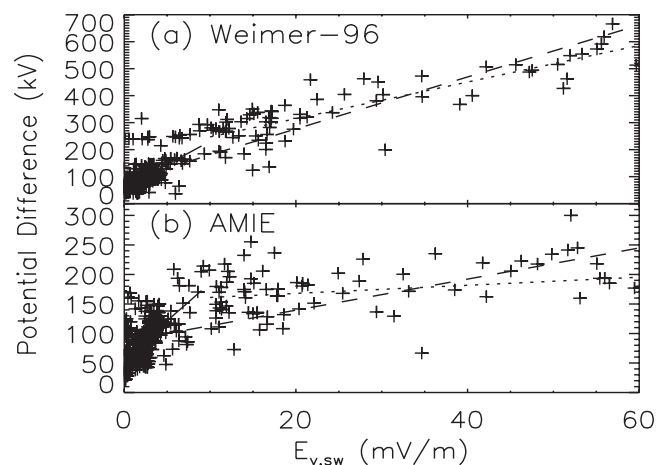


**Figure 3.**  $\Delta\Phi_{PC}$  versus  $E_{y,sw}$  for (a) Weimer-96 and (b) AMIE. Note the y-axis scales are different. Also shown are linear fits to subsets of the data (see text and Table 1).

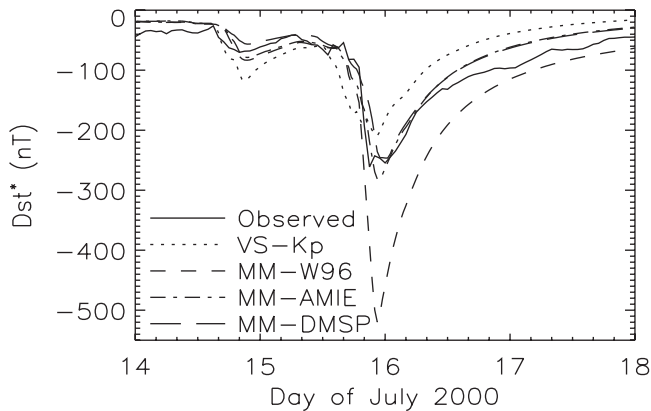


**Figure 4.** Observed (solid line) and simulated (other lines)  $Dst^*$  values during this period.

values. The solid line is a linear regression fit to the data with  $E_{y,sw} = [0,10]$ , the dotted line is a fit for  $E_{y,sw} = [10,60]$ , and the dashed line is a fit of the entire range shown. The results of these fits are given in Table 1. The correlation coefficients  $R$  indicate that the W-96 model is linear with large values of  $E_{y,sw}$  while the AMIE results are not. At low  $E_{y,sw}$ , other factors become significant in the determination of  $\Delta\Phi_{PC}$  (e.g.,  $B_{y,IMF}$ ), and the correlation goes down. Uncertainties associated with the time lag applied to the solar wind measurements from ACE and the time lag in the magnetospheric response to solar wind variations (up to 30 min) only change the  $R$  values by 0.02 at most.

### 3. Ring Current Results

[12] The purpose of this study is to examine whether the inner magnetosphere also shows evidence of a nonlinear response to extreme  $E_{y,sw}$ . To do this, a bounce-averaged kinetic model of hot ion transport is used. Developed over the last decade, this model uses a finite volume numerical approach to solve for the phase space distribution of a particular plasma species ( $H^+$  and  $O^+$  for these calculations) as a function of time, equatorial plane geocentric distance, local time, kinetic energy, and equatorial pitch angle. The plasma source is specified by nightside ion flux measurements from several geosynchronously-orbiting spacecraft (data from 4 satellites were used in these calculations). Please see *Liemohn et al.* [2001] for further details of the model description and the validity of this ring current simulation technique.

[13] Figure 4 shows the observed  $Dst^*$  along with  $Dst^*$  values from several numerical simulations. The model  $Dst^*$  values are found from the Dessler-Parker-Sckopke (DPS) relation [*Dessler and Parker, 1959; Sckopke, 1966*], which relates the total energy content of the plasma in near-Earth space to the resulting globally-averaged magnetic perturbation. By choosing this comparison, it is assumed that  $Dst^*$  is caused primarily by the magnetospheric

**Table 1.** Linear Regression Results<sup>a</sup>

Method	$E_{y,sw}$ Range	b	m	R
W-96	[0,10]	60.1	17.1	0.618
W-96	[10,60]	180.	6.78	0.859
W-96	[0,60]	84.1	9.63	0.905
AMIE	[0,10]	57.7	12.8	0.640
AMIE	[10,60]	154.	0.686	0.256
AMIE	[0,60]	86.9	2.63	0.626

<sup>a</sup>  $\Delta\Phi_{PC} = b + mE_{y,sw}$  with correlation coefficient  $R$ .

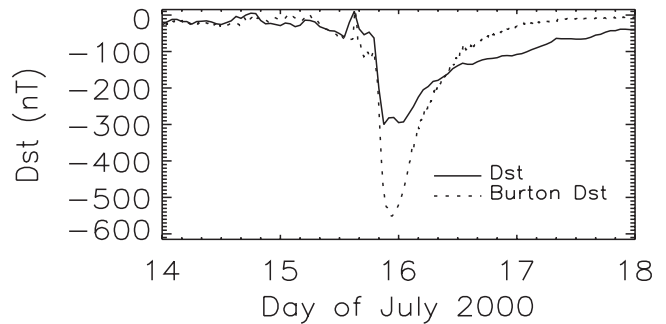


**Figure 5.**  $Dst$  values for the storm from observations (solid line) and predictions (dotted line) from the *Burton et al.* [1975] algorithm.

component of the ring current, an approximation supported by recent observational studies [e.g., *Greenspan and Hamilton, 2000*]. The linearity assumption of the DPS relation is another source of uncertainty (up to 30% [*Carovillano and Siscoe, 1973*]), but the inflation would also increase the distance of the ring current from the planet, canceling some of this effect.

[14] The only difference between the simulations shown in Figure 4 is in the magnetospheric convection electric field description. The first uses a shielded Volland-Stern (VS designation) electric field driven by the 3-h Kp index. The other 3 use the modified McIlwain electric field pattern (MM designation) [see *Liemohn et al., 2001*], which is driven by  $\Delta\Phi_{PC}$ . The 3 simulations use the W-96 values, the AMIE values, and the DMSP values (results using W2K are not shown, since its  $\Delta\Phi_{PC}$  was so similar to W-96).

[15] The simulation driven by the W-96  $\Delta\Phi_{PC}$  values (MM-W96) does not reproduce the observed  $Dst^*$ . Both minima are too deep, with the second one reaching  $-520$  nT (twice the observed value). The other 3 simulation results come much closer to the observed values (within the uncertainty of the  $Dst^*$ -ring current energy assumption). The closeness of the VS-Kp simulation's  $Dst^*$  minimum to the observed minimum is because the chosen activity dependence of this electric field [from *Maynard and Chen, 1975*] saturates for large Kp.

[16] The question of why the MM-W96 simulation did not reproduce the observed  $Dst^*$  values can be addressed by considering the numbers in Table 2. It is seen that the VS-Kp simulation has the largest total energy inflow through the outer boundary (integrated from 1200 UT on July 14 to 1200 UT on July 16). The difference is not with the inflow but rather with the net energy gain due to adiabatic acceleration within the computational domain. Net adiabatic energization for MM-W96 is twice the size as that from the other simulations. Therefore, the extra magnetic perturbation ( $Dst^*$ ) is caused largely by the ions being pushed closer to the Earth during their inner magnetospheric traversal.

[17] The conclusion of *Russell et al.* [2001] that the inner magnetospheric hot particle population scales linearly with  $E_{y,sw}$  is based chiefly on the accuracy of the  $Dst$  prediction algorithm of *Burton et al.* [1975]. This method linearly scales the rate of  $Dst$  decrease (ring current growth) with  $E_{y,sw}$ . Figure 5 shows the comparison between the observed  $Dst$  and the *Burton et al.* prediction. The *Burton et al.*  $Dst$  reaches  $-551$  nT, nearly double the amplitude of the observed minimum value. This discrepancy is very consistent with the ring current simulation results.

### 4. Conclusions

[18] For the Bastille Day storm of 2000,  $\Delta\Phi_{PC}$  exhibited a nonlinear saturation in its response to the extreme solar wind conditions. The ring current simulation with an unsaturated convection strength overpredicted the intensity of the storm by a factor

**Table 2.** Simulation Results

	VS-Kp	MM-W96	MM-AMIE	MM-DMSP
Minimum Dst*, nT	-209.	-520.	-281.	-246.
Total Energy Inflow, PJ	24.2	19.7	14.7	11.9
Total Net Adiabatic Energy Gain, PJ	10.3	23.3	12.3	11.1
Peak $E_{v,conv}$ at L=6.6, MLT=00, mV/m	1.41	4.02	1.77	1.47

of 2, while the others did not. This large discrepancy is much larger than any uncertainty in comparing the ring current strength with Dst\*. Similarly, the *Burton et al.* [1975] prediction algorithm overshoot the Dst minimum by a factor of 2. These results support the concept of asymptotic ring current intensity during extreme solar wind conditions.

[19] There are two leading possibilities for the cause of the nonlinearity. The first is the feedback from the region 1 current system on the subsolar reconnection rate [*Hill et al.*, 1976]. The second is the nightside, mid-latitude potential pattern (driven by the closure currents of the stormtime partial ring current), which effectively reduces the convection strength in the near-Earth plasma sheet [*Ridley and Liemohn*, 2002]. Future studies will examine these mechanisms.

[20] **Acknowledgments.** This work was supported by NASA grants NAG5-4771, NAG5-10297, and NAG-10850, and NSF contracts ATM-9711381, ATM-9800830, and ATM-0090165. Supply of the DMSP data was supported by NASA grant NAG5-9297. The authors would also like to thank all of the data providers that make the ring current simulations possible, particularly Michelle Thomsen and Geoff Reeves at Los Alamos National Laboratory, the ACE particle and field instrument teams and CDAWeb for access to this data, and the Kyoto World Data Center.

## References

- Boyle, C. B., P. H. Reiff, and M. R. Hairston, Empirical polar cap potentials, *J. Geophys. Res.*, *102*, 111, 1997.
- Burke, W. J., D. R. Weimer, and N. C. Maynard, Geoeffective interplanetary scale sizes derived from regression analysis of polar cap potentials, *J. Geophys. Res.*, *104*, 9989, 1999.
- Burton, R. K., R. L. McPherron, and C. T. Russell, An empirical relationship between interplanetary conditions and Dst, *J. Geophys. Res.*, *80*, 4204-4214, 1975.
- Carovillano, R. L., and G. L. Siscoe, Energy and momentum theorems in magnetospheric processes, *Rev. of Geophys. Space Phys.*, *11*, 289, 1973.
- Cole, K. D., Damping of magnetospheric motions by the ionosphere, *J. Geophys. Res.*, *68*, 3231, 1963.
- Dessler, A. J., and E. N. Parker, Hydromagnetic theory of geomagnetic storms, *J. Geophys. Res.*, *64*, 2239, 1959.
- Greenspan, M. E., and D. C. Hamilton, A test of the Dessler-Parker-Sckopke relation during magnetic storms, *J. Geophys. Res.*, *105*, 5419, 2000.
- Hairston, M. R., and R. A. Heelis, Analysis of ionospheric parameters based on DMSP SSIES data using the DBASE4 and NADIA programs, *Tech. Rep. PL-TR-96-2078*, Phillips Laboratory, Hanscom Air Force Base, Mass., 1996.
- Hairston, M. R., R. A. Heelis, and T. W. Hill, Observed saturation of the ionospheric cross polar cap potential during the 31 March 2001 storm, *Eos Trans. AGU*, *82*(47), 2001 Fall Meet. Suppl., F1055, 2001.
- Hill, T. W., A. J. Dessler, and R. A. Wolf, Mercury and Mars: The role of

- ionospheric conductivity in the acceleration of magnetospheric particles, *Geophys. Res. Lett.*, *3*, 429, 1976.
- Kozyra, J. U., V. K. Jordanova, J. E. Borovsky, M. F. Thomsen, D. J. Knipp, D. S. Evans, D. J. McComas, and T. E. Cayton, Effects of a high-density plasma sheet on ring current development during the November 2-6, 1993, magnetic storm, *J. Geophys. Res.*, *103*, 26,285, 1998.
- Liemohn, M. W., J. U. Kozyra, M. F. Thomsen, J. L. Roeder, G. Lu, J. E. Borovsky, and T. E. Cayton, The dominant role of the asymmetric ring current in producing the stormtime Dst\*, *J. Geophys. Res.*, *106*, 10,883, 2001.
- Maynard, N. C., and A. J. Chen, Isolated cold plasma regions: Observations and their relation to possible production mechanisms, *J. Geophys. Res.*, *80*, 1009, 1975.
- Reiff, P. H., R. W. Spiro, and T. W. Hill, Dependence of polar cap potential drop of interplanetary parameters, *J. Geophys. Res.*, *86*, 7639, 1981.
- Rich, F. J., and M. R. Hairston, Large-scale convection patterns observed by DMSP, *J. Geophys. Res.*, *99*, 3827, 1994.
- Richmond, A. D., and Y. Kamide, Mapping electrodynamic features of the high-latitude ionosphere from localized observations: Technique, *J. Geophys. Res.*, *93*, 5741, 1988.
- Ridley, A. J., and M. W. Liemohn, A model-derived description of the penetration electric field, *J. Geophys. Res.*, *107*, in press, 2002.
- Russell, C. T., J. G. Luhmann, and G. Lu, Nonlinear response of the polar ionosphere to large values of the interplanetary electric field, *J. Geophys. Res.*, *106*, 18,495, 2001.
- Sckopke, N., A general relation between the energy of trapped particles and the disturbance field near the Earth, *J. Geophys. Res.*, *71*, 3125, 1966.
- Siscoe, G. L., G. M. Erickson, B. U. Ö. Sonnerup, N. C. Maynard, J. A. Schoendorf, K. D. Siebert, D. R. Weimer, W. W. White, and G. R. Wilson, Region 1 current-voltage relation: Test of Hill model, saturation, and dipole-strength scaling, submitted to *J. Geophys. Res.*, 2001.
- Weimer, D. R., A flexible, IMF dependent model of high latitude electric potentials having "space weather" applications, *Geophys. Res. Lett.*, *23*, 2549, 1996.
- Weimer, D. R., An improved model of ionospheric electric potentials including substorm perturbations and application to the Geospace Environment Modeling November 24, 1996, event, *J. Geophys. Res.*, *106*, 407, 2001.

J. U. Kozyra, M. W. Liemohn, A. J. Ridley, and T. H. Zurbuchen, Space Physics Research Laboratory, University of Michigan, Ann Arbor, MI 48109-2143, USA. (liemohn@umich.edu).

M. R. Hairston, Center for Space Science, University of Texas at Dallas, Richardson, TX 75083-0688, USA. (hairston@utdallas.edu).

D. R. Weimer, Mission Research Corporation, 589 W. Hollis St., Suite 201, Nashua, NH 03062, USA. (dweimer@mrcnh.com).

G. Lu, High Altitude Observatory, NCAR, 3450 Mitchell Lane, Boulder, CO 80307-3000, USA. (ganglu@ucar.edu).

R. M. Skoug, Los Alamos National Laboratory, NIS-1 MS D466, Los Alamos, NM 87545, USA. (rskoug@lanl.gov).